Environ Monit Assess (2023) 195:1496
https://doi.org/10.1007/s10661-023-12086-9

RESEARCH

Agricultural abandoned lands as emission sources of dust containing metals and pesticides in the Sonora-Arizona Desert

Jesús Arturo Bracamonte-Terán · Diana Meza-Figueroa · Leticia García-Rico · Benedetto Schiavo · María Mercedes Meza-Montenegro · Ana Isabel Valenzuela-Quintanar

Received: 18 August 2023 / Accepted: 2 November 2023 / Published online: 20 November 2023

Abstract This investigation examines the transport of metal- and pesticide-polluted dust emitted by one of the most relevant agricultural areas of Northwestern Mexico. In the contaminated area, an excessive water extraction of the aquifer and seawater intrusion caused the abandonment of fields, which are pollutant-loaded dust emitters. We used air mass forward trajectories (HYSPLIT) model to obtain particle trajectories in the wind and the use of banned pesticides as geochemical tracers for dust transported by wind. Fifty dust samples from 10 agriculture fields and 26 roof dust of a city close to the agricultural area were analyzed for their contents of zirconium, lead, arsenic, zinc, copper, iron, manganese, vanadium, and titanium, by portable X-ray fluorescence. Nine pesticides were analyzed in the roof dust and agricultural soil samples by gas chromatography. Results show that the distribution of metals was significantly different between active and abandoned fields. Arsenic-lead-copper was mainly concentrated in abandoned fields, while zinc-iron-manganese-titanium was dominant in active fields. Two potential sources of metal contamination were found by principal component analysis (PCA): (I) a mixture of traffic and agricultural sources and (II) a group related to agricultural activities. The occurrence of banned pesticides in dust deposited on roofs collected at nearby cities confirms the atmospheric transport from the agricultural area. The HYSPLIT results indicated that the dust emitted from agricultural fields can reach up to the neighboring states of Sonora, Mexico, and the USA. The impacts that these emissions can have on human health should be studied in future research.

J.A. Bracamonte-Terán, D. Meza-Figueroa, and L. García-Rico contributed equally to this work and share the first authorship.

Supplementary Information The online version contains supplementary material available at https://doi.org/10.1007/s10661-023-12086-9.

J. A. Bracamonte-Terán
Programa de Doctorado en Ciencias, Centro de Investigación en Alimentación y Desarrollo A.C. Carretera Gustavo E. Astiazarán Rosas 46, La Victoria, 83304 Hermosillo, Mexico

D. Meza-Figueroa (✉)
División de Ciencias Exactas y Naturales, Departamento de Geología, Universidad de Sonora, Rosales y Encinas, 83000 Hermosillo, Mexico
e-mail: diana.meza@unison.mx

L. García-Rico (✉) · A. I. Valenzuela-Quintanar
Centro de Investigación en Alimentación y Desarrollo A.C. Carretera Gustavo E. Astiazarán Rosas 46, La Victoria, 83304 Hermosillo, Mexico
e-mail: lgarciar@ciad.mx

B. Schiavo
Instituto de Geofísica, Universidad Nacional Autónoma de México, Mexico City, Mexico

M. M. Meza-Montenegro
Departamento de Recursos Naturales, Instituto Tecnológico de Sonora, 5 de Febrero 818 Sur, 85000 Cd. Obregón, Mexico

Keywords Metals · Arid zones · Agricultural soils · Dust transport · HYSPLIT

Introduction

Agricultural lands are essential resources for food production, so applying techniques to improve their use is essential to meet the growing food demand. However, the development of farming practices aimed at higher profits and lower costs has increased the use of chemicals. Therefore, the implementation of unsustainable agricultural land management has caused soil degradation in many areas worldwide (IPCC, 2019). Intensive agricultural practices reduce the damage to crops by pests (e.g., insects, weeds, fungi, and rodents) but affect the soil's fertility and its productive capacity (Alengebawy et al., 2021). Consequently, bare lands with poor soil structure are abandoned and further exposed to aeolian erosion. Due to such processes, agricultural lands become anthropogenic dust sources and emitters generating atmospheric hazards (Chalise et al., 2019; Katra, 2020; Vimic et al., 2021). Previous studies in the nearby Arizona region indicate that 51 to 55% of PM_{10} in the city of Phoenix comes from erosion of nearby croplands (Joshi, 2021).

Because degraded farmed soils tend to have finer particles, they become a major dust emitter in arid environments (Pozzer et al., 2017; Zeb et al., 2022). Low soil moisture and a high percentage of silt and clay are important factors for transporting pollutants associated with agriculture (Péterfalvi et al., 2018; Singh et al., 2021). Dust emissions in agricultural fields (IPCC, 2019; Wagari & Tamiru, 2021) located in desert environments impact air quality due to fine particles that have a long residence time in the atmosphere (Pi et al., 2022). The Hermosillo Coast area (HCA) has been one of Mexico's most relevant agricultural districts since 1945 (Ochoa-Noriega et al., 2022). Currently, Sonora is the leading producer of table grapes in Mexico, contributing to more than 80% of the country's production. Mexico now accounts for 6% of world table grape exports. Most of this region's production is exported to 30 countries, the most important of which is the USA, due to competitive advantages such as geographic proximity and the commercial window of this country (SIAP, 2021). The HCA is an area that is sustained by the exploitation of an aquifer in which water extraction has historically exceeded recharge because of the climate characteristics of the Sonora-Arizona desert. Freshwater extraction for agricultural use has resulted in seawater intrusion problems near the coastline (Zepeda et al., 2018). Due to high salt concentrations in the wells, agricultural fields have been abandoned (Ochoa-Noriega et al., 2022), and due to the lack of vegetative cover, these fields are highly erodible. In addition, because of the long history of agrochemical's overuse in the region, the soils are loaded with organochlorides, fertilizers, arsenic/lead bases, and metals (Leal et al., 2014; Meza-Montenegro et al., 2013).

Different studies have been carried out in the region of HCA, and most of them have focused on the sustainable use of water and land (Ochoa-Noriega et al., 2022; Zepeda et al., 2018). However, scarce research has reported soil/dust contaminants related to agricultural fields of the region (Leal et al., 2014; Meza-Montenegro et al., 2012, 2013; Moreno-Rodríguez et al., 2020), and none have focused on assessing the source of pollutant emissions and transport to nearby communities.

Polluted dust by metals and pesticides has been associated with the development of cancer in exposed populations (Alengebawy et al., 2021; Chen et al., 2021), but also dust can carry fungus spores associated with valley fever by the aeolian erosion of soil-dwelling *Coccidioides immitis* and *Coccidioides posadasii* (Sprigg et al., 2014). Therefore, the identification of sources and the transport mechanisms of contaminants is essential to mitigate the emission of polluted dust from agricultural soils. Pesticides are potential carcinogens that are persistent in the environment and accumulate in agricultural soils (Alengebawy et al., 2021; Chen et al., 2021). For these reasons, organochloride pesticides (OCPs) such as p,p′-dichlorodiphenyltrichloroethane (DDT), endosulfan, hexachlorobenzene (HCB), and heptachlor, including herbicide glyphosate, have been banned in different countries (Chen et al., 2021). Many of these pesticides are degraded in soil by microorganisms and transformed into metabolites (for example, DDT to DDE (p,p′-dichlorodiphenyldichloroethane), glyphosate to aminomethylphosphonic acid (AMPA)), which decay rates are lower than their parent compounds and therefore persist in soils in higher levels for a long time (Ramirez et al., 2021).

There are other techniques that evaluate the transport of metals in dust (e.g., analysis of meteorological

data, satellite images and remote sensing, spatial modeling, geological tracers, among others) (Baltas et al., 2020; González-Guzmán et al., 2022). The most used of these models is probably the Hybrid Single Particle Lagrangian Integrated Trajectory (HYSPLIT) model. By using HYSPLIT forward-backward trajectory analysis, it is possible to trace the transport and diffusion of air masses (Wang et al., 2019). These models have been recently used along with other analytical tools (e.g., positive matrix factorization, X-ray fluorescence, multivariate analysis) (Attiya & Jones, 2020; Luo et al., 2020; Miglioranza et al., 2021; Singh et al., 2021) to trace the origin of metal emissions more accurately. Although HYSPLIT and geochemical tracers are widely applied in metal studies (Jooybari et al., 2022), they have rarely been used for source apportionment of polluted dust released at agricultural areas.

The objectives of this study were the following: (i) to determine the concentration of metals and pesticides in active and abandoned agricultural soils and settled dust collected at schools' roofs and (ii) to determine the environmental fate of polluted dust in nearby settlements using HYSPLIT, PCA, metals, and pesticides as geochemical tracers.

Methodology

Site description

The HCA study area is in Northwestern Mexico, in the state of Sonora, facing the Gulf of California (Fig. 1). Agricultural activity is sustained by water extracted from the Hermosillo aquifer, which has the largest deficit of any water body in the region. The climate is semi-arid with an average annual temperature of 24 °C with minimum temperatures of −3 °C and maximum temperatures of 46 °C, with average annual precipitation of 200 mm (Salazar-Adams et al., 2012). Wind patterns in the region are influenced by the North American Monsoon (Ochoa-Noriega et al., 2022). Soils are vast alluvial deposits with a mixture of clay (45%), silt (35%), and sand (20%) fractions (Leal et al., 2014, Table 1).

The HCA ranks third in volume of agricultural production in the state of Sonora with a value of 173 million dollars. The predominant crops are tomato, pumpkin, asparagus, green chili, melon, citrus, cucumber, watermelon, grapes, and walnuts, which are mainly exported (SIAP, 2021). In the early 1940s, the HCA experienced a socioeconomic

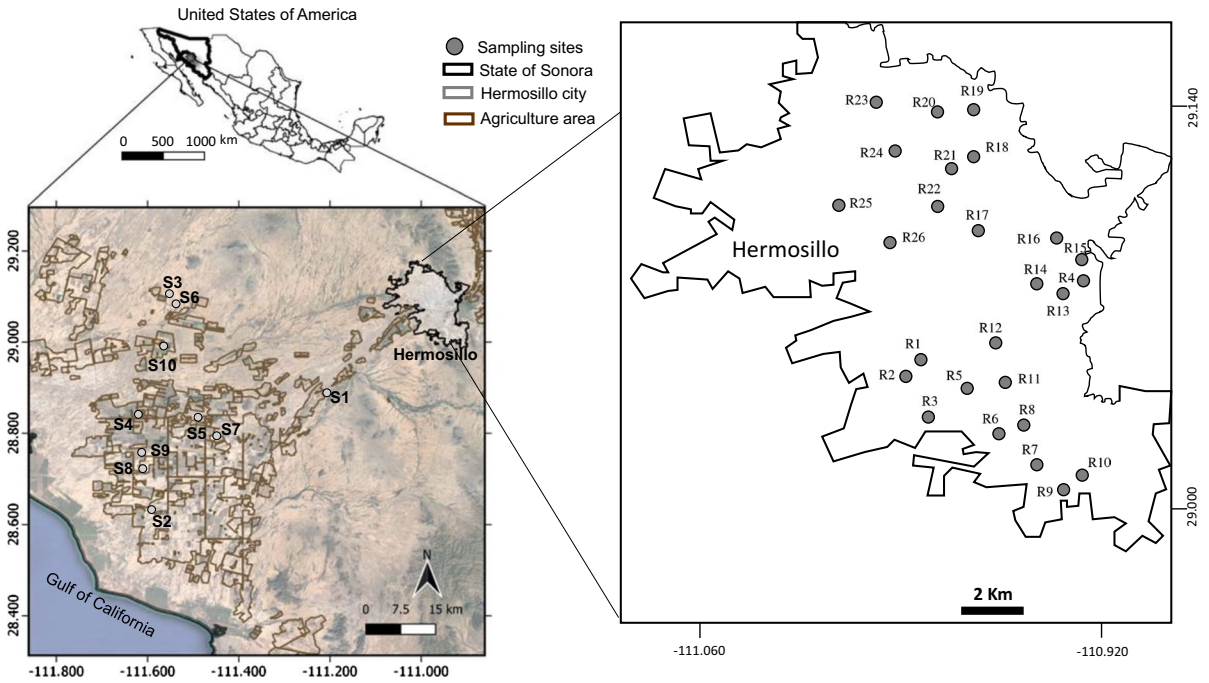

Fig. 1 Location of the sampling points in the agricultural fields of the Hermosillo Coast area (HCA)

Table 1 Location of agricultural fields from the Hermosillo Coast area (HCA). *Data from Leal et al. (2014)

Site	Coordinates	Distance to Hermosillo city (km)	Status	Initiation of cropping	Current crop	Historical crops	Surface (Ha)	Organic matter *(%)	Coarse sand *(%)	Fine sand *(%)	Silt and clay *(%)
S1	28.894–110.768	31.44	Active	1940	Cantaloupe, watermelon	Cotton, wheat	200	0.70	19.79	66.39	13.82
S2	28.633–110.387	78.59	Active	1977	Chickpea	Cotton, wheat, grape, orange	500	3.88	13.02	86.79	0.18
S3	29.112–110.271	57.45	Abandoned	1950	-	Cotton, wheat, safflower, walnut, grape	90	1.55	4.37	84.60	11.03
S4	28.845–110.350	69.47	Abandoned	1950	-	Cotton, wheat, chickpea, corn	900	4.45	10.09	72.22	17.70
S5	28.836–110.479	58.55	Abandoned	1950	-	Cotton	50	2.73	4.70	82.68	12.62
S6	29.094–110.429	56.62	Active	1970	Grape	Cotton, wheat, walnut, grape, safflower, beans, citrus	400	0.95	37.12	57.75	5.13
S7	28.792–110.521	57.53	Active	1960	Wheat, chickpea	Cotton, wheat, walnut, grape	2000	0.58	47.95	44.37	7.68
S8	28.721–110.359	75.08	Abandoned	1950	-	Cotton	500	1.01	1.20	81.52	17.26
S9	28.764–110.358	72.65	Abandoned	1935	-	Cotton, grape, walnut	400	1.97	64.90	34.53	0.57
S10	28.996–110.405	59.72	Active	1998	Peach	Grape, walnut	1000	0.82	37.77	62.01	0.22

and agricultural boom. The increase in land used for agriculture demands larger volumes of groundwater, resulting in seawater intrusion into most agricultural fields (Ochoa-Noriega et al., 2022; Zepeda et al., 2018). Nowadays, much of the region contains patches of degraded-abandoned land, which are susceptible to erosion (Moreno-Rodríguez et al., 2020). Thus, these lands are important dust emitters.

Sampling, processing, and analysis

Soil samples from ten agricultural fields were provided by the authors of the study by Leal et al. (2014), and the sampling methods are described in that work. In addition, 26 settled dust samples from school roofs in Hermosillo city were obtained by sweeping an area of 2 m^2 and were collected using plastic tools, transported in polyethylene bags, and stored at −20 °C until analysis (Meza-Figueroa et al., 2020). Roof dust samples were collected in accordance with careful sweeping dry deposition procedures previously described by Lee et al. (2020) and Candeias et al. (2021). In this study, the samples represent dust settled by dry atmospheric deposition. In the city, it only rains in the monsoon season (summer) and occasionally during winter (December). Because the city has a semi-desert climate, the dust collected would represent atmospheric pollution for dry months (January to June). For OCPs and metal analysis, soil and dust samples were homogenized, air-dried at room temperature, and oven-dried at 35 °C for 24 h, respectively (Leal et al., 2014; NMX-AA-132-SCFI-2016, 2016). Then, samples were sieved using a Ro-Tap Tyler Model RX-86, and the final fraction that passed through the mesh at sequence: #18, #120, #230, #325, #635 mesh was used for geochemical analysis. The #635 mesh fraction (<20 μm in aerodynamic diameter) is the most likely to be suspended by the wind and to be transported to more sensitive areas.

Total concentration of zirconium (Zr), lead (Pb), arsenic (As), zinc (Zn), copper (Cu), iron (Fe), manganese (Mn), vanadium (V), and titanium (Ti) was analyzed in homogenized soil and dust samples (< 20 μm) by a portable X-ray fluorescence (PXRF) analyzer (Niton FXL GOLDD, Thermo Scientific, Inc., MA, USA), following the method 6200 of the US Environmental Protection Agency (USEPA, 2007). Previous studies have shown the efficiency of this technique for the analysis of dusts (Fry et al., 2021; Spada et al., 2023). Silicon dioxide was used as a blank, and triplicate measurements per sample were performed during 120 s. The precision (RSD) and accuracy (%) were <20% considering seven replicates of the standard reference materials (SRM) 2710a and 2711a from the National Institute of Standards and Technology (NIST) (Table S1). To ensure the quality of the data, reference material SRM 2710a was measured every ten samples, and the average recoveries of the study elements were between 90 and 110%. Detection limits for analyzed metals are (mg kg^{-1}) as follows: Zr (2), Pb (2), As (2), Zn (4), Cu (6), Fe (20), Mn (12), V (8), and Ti (10).

The extraction and quantification of OCPs in settled dust at school roofs were performed by matrix solid-phase dispersion and gas chromatograph (MSPD) (7890A system, equipped with an electron micro-capture detector and 7683B series injector autosampler, Agilent Technologies) (Leal et al., 2014; Meza-Montenegro et al., 2013). A DB-5 capillary column (30 m × 0.250 mm × 0.25 μm) was used. The oven temperature program was initially at 110 °C (1 min), with a final 280 °C (2 min) (rate, 15 °C min up to 280 °C). Injector temperature was 270 °C operated in splitless injection of 1 mL. Helium was used as the carrier gas at 2.3 mL min^{-1} under constant flow mode. The extraction and quantification of OCPs were based according to Leal et al. (2014). Briefly, the aluminum oxide was inactivated at 900 °C for 12 h and then adjusted to 9% moisture. Dust samples (0.5 g) were place in a mortar and ground with 0.6 g of aluminum oxide for the dispersion. For the purification of the sample, 5 mL glass syringe was packed at the bottom with glass fiber and 2.6 g aluminum oxide. The dispersed dust sample was added to the column, and the OCPs in the sample were eluted with 40 mL of hexane. The eluate was collected in 50-mL conical glass tube and evaporated to dryness with dry air with compressed air (N-EPAP 11155RT Model, Organomation Associates, MA, USA). The concentrate was reconstituted with 100 mL of hexane. All OPCs analyses included a blank sample or negative control, a sample added or positive control (dust spiked with of a mixture of OCPs known concentration). The detection limits for all OCPs were between 0.2 and 0.5 μg kg^{-1}; the accuracy and precision were from 84 to 101% and <18%, respectively.

Forward air trajectory analysis

HYSPLIT model developed by the National Oceanic and Atmospheric Administration (NOAA) of the USA was used to compute the meteorological information and air mass trajectories. A forward trajectory model was performed to detect the route of transported metal-dust from the HCA. The HYSPLIT trajectory model is a simple and powerful tool to investigate airflow patterns. For this work, the meteorological information was obtained from NCEP (National Center for Environmental Prediction, USA) data sets, which contain reanalysis data, and Global Data Set Assimilation System (GDAS) data at a resolution of 0.5 km. The active and abandoned agricultural fields ($n = 5$) of HCA with the highest percentages of silt and clay were selected as starting point for the forward trajectory model (Table 1). Forward trajectories from site 1, site 3, site 4, site 5, and site 8 were calculated on dates prior to monsoon season for 5 days in 2014: March 01 and 11 and April 08, 20, and 21 (starting at 1700 UTC) during 24 h at three different heights—250, 300, and 350 m above ground level. These altitudes were selected since at these heights dust particles can be lifted and transported over long distances. The trajectories were computed using the Real Time Environmental Applications and Display sYstem (González-Guzmán et al., 2022; Miglioranza et al., 2021). The dates for modeling particle trajectories were chosen based on the work of Meza-Figueroa et al. (2016), where it is reported that dusty days (those exceeding the historical average of suspended particulate matter) occur mainly between October–December and April–June. Moreno-Rodríguez et al. (2015) report that the main wind direction is SW-NE with slight variations S-N (data based on a record from 2000 to 2012). The maximum wind speed is 6.1 m s^{-1} during the period from April to June (Moreno-Rodríguez et al., 2015).

Statistical analysis and geographic information system

All data distributions were performed for normality using Shapiro-Wilk test. Descriptive statistics were used. Correlation analysis between the metal-metal and metal-pesticide contents in soil and dust samples was calculated using Spearman's correlations. The identification of common source of metals was performed by PCA using XLSTAT software 24.1.1283.0. Significant differences between sites were evaluated according to the Kruskal-Wallis Multiple-Comparison Z-Value Test and were performed using NCSS version 21.01.3. Results with $p < 0.05$ were considered statistically significant. The Kaiser-Meyer-Olkin measure (0.7) and Bartlett's test of sphericity indicate that PCA is feasible for the dataset. Finally, statistical information was plotted using XLSTAT software 24.1.1283.0 and interpolated using Geographical Information System QGIS free software to generate maps.

Results and discussion

Soil physicochemical parameters

The agricultural soils studied have a clay and silt percentage ranging from 0.18 to 17.70% (Table 1). The highest percentages of silt and clay were obtained in abandoned sites S3 (11.03%), S5 (12.62%), S4 (17.7 %), and S8 (17.26 %), indicating that these sites are more susceptible to wind erosion and airborne dust transport. For the active agricultural fields, the highest value corresponds to site S1 (13.82 %), while the rest of the active fields have a range of clay and silt from 0.18 to 7.68%. The content of organic matter (OM) in soils also may contribute to the accumulation of metals and agrochemicals. The role of OM in metal availability has been widely investigated. It has been reported that metal accumulation in soil decreased as OM levels decrease (Avendaño et al., 2021). The OM levels in agricultural soil samples from HCA ranged from 0.58 to 4.45% (Table 1). The site with the highest OM concentration was S4 (4.45%), a field that was recently abandoned and which also had the highest levels of Pb, As, and Cu.

Metal concentrations in agricultural soils and dust settled on roofs

The mean metal levels detected in the studied agricultural soils ($n = 50$) and settled dust at roofs ($n = 26$) are shown in Tables 2 and 3 and Table S2. The most abundant element was Fe,

followed by Ti, Mn, Zr, V, Cu, Pb, and As. Fe along with Ti are major elements in soils and are part of the structural formula of rock-forming minerals; therefore, they are commonly associated with a

Table 2 Metal content in agricultural soils worldwide (range and mean values in mg kg^{-1}). Abbreviations are No reported (NR)

Locality	Zr	Pb	As	Zn	Cu	Fe	Mn	V	Ti	Reference
Hermosillo Coast area										Present study
Min	180.7	2.5	4.1	65.9	29.6	26,240.8	426.8	79.8	2679.8	
Max	849.2	60.6	44.0	316.7	119.3	85,107.2	2731.4	152.2	6939.2	
Mean	354.3	24.7	19.3	154.0	54.1	43,281.9	1022.2	104.0	3800.5	
%CV	43.1	84.2	48.2	42.8	35.8	36.5	66.3	14.8	24.8	
Dhaka district, Bangladesh	NR NR	41–87.5 65.98	10.5–45 20.3	32.5–80 53.3	35–91 57.2	8085–22,455 12,232	198–755 455.4	NR NR	NR NR	Bhuiyan et al. (2021)
Shanghai, China	NR NR	19.7–27.4 24.2	6.3–7.4 6.97	NR NR	NR NR	NR NR	NR NR	NR NR	NR NR	Fei et al. (2022)
Yunnan Province, Southwest China	NR NR	8.3–258.8 64.5	9.3–293.3 50.7	28.5–595.5 120	15.8–143.8 43.8	NR NR	107–1593 548	39.8–278.8 105.1	NR NR	Wang et al. (2021)
Europe	NR	5–150	2–300	15–350	NR	NR	NR	NR	NR	Tóth et al. (2016)
Huabei plain, north China	NR NR	12.7–54.9 30.4	3.0–12.8 6.8	27.5–188.9 72.1	9.4–72.6 27.7	NR NR	NR NR	NR NR	NR NR	Huang and Jin (2008)
Greece	NR NR	3.2–48.5 19.7	2.7–12.8 6.95	23–288.5 74.9	11.9–653 74.7	12,800–40,500 26,200	267–3495 1020.5	NR NR	NR NR	Kelepertzis (2014)
Shiraz, Iran	NR	254.6	NR	117	96.9	NR	NR	NR	NR	Qishlaqui and Moore (2007)

Table 3 Metal levels in soils from agricultural fields and settled dust in roofs (mg kg^{-1}). Different letter by row means significant different (Kruskal-Wallis, $p < 0.05$)

Element		Agricultural soils		Roofs
		Active ($n = 25$)	Abandoned ($n = 25$)	Settled dust ($n = 26$)
Zr	Min–max	184.9–761.1	180.7–849.1	5–585.3
	Mean ± SD	412.0 ± 145.7	296.6 ± 140.6	197.1 ± 232.3
	Median	478.7[a]	241.7[b]	5.0
	%CV	35.1	47.4	84.8
Pb	Min–max	2.5–54.5	2.5–60.6	10.2–236.7
	Mean ± SD	27.1 ± 17.9	22.3 ± 23.5	53.9 ± 46.2
	Median	33.0	2.5	39.0
	%CV	66.0	105.1	116.5
As	Min–max	7.5–29.7	4.1–44.0	5–15.8
	Mean ± SD	18.4 ± 6.5	20.3 ± 11.5	7.2 ± 4.0
	Median	18.5	17.9	5.0
	%CV	35.3	56.9	177.0
Zn	Min–max	88.3–295.9	65.9–316.7	70.5–3102
	Mean ± SD	162.5 ± 65.3	145.4 ± 66.8	506.0 ± 706.3
	Median	134.9	121.3	199.8
	%CV	40.2	46.0	71.6
Cu	Min–max	33.1–79.7	29.6–119.3	10.7–214.4
	Mean ± SD	54.1 ± 13.1	54.2 ± 24.4	66.2 ± 58.8
	Median	51.0	42.9	47.3
	%CV	24.2	45.0	112.6
Fe	Min–max	28,018.1–85,107.2	26,240.8–80,412.0	1089–31,544
	Mean ± SD	46,491.2 ± 16,966.3	40072.6 ± 14142.1	12,851 ± 12,472.3
	Median	39,968.0	35,446.4	3418.8
	%CV	36.5	35.3	103.1
Mn	Min–max	448.6–2444.3	426.8–2731.4	5–636
	Mean ± SD	1117.0 ± 690.1	927.4 ± 665.5	168.9 ± 235.0
	Median	745.4	589.9	5.0
	%CV	61.8	71.8	71.9
V	Min–max	79.8–152.2	81.0–136.0	2.3–305
	Mean ± SD	106.6 ± 16.8	101.3 ± 13.7	62.9 ± 106.4
	Median	101.0	96.6	6.6
	%CV	15.8	13.5	59.1
Ti	Min–max	6939.2–2785.2	2679.8–6123.0	5–20087
	Mean ± SD	4102.6 ± 1046.9	3498.4 ± 722.2	2667.4 ± 4299.7
	Median	3708.0[a]	3328.7[b]	5.0
	%CV	25.5	20.6	62.0

crustal origin (Taylor, 1964). However, Pb, Zn, and Ti appear in higher concentrations in dust deposited on roofs (Table S2) as they are contaminants mainly associated with the urban environment due to traffic activity and urban erosion (Gallego-Hernández et al., 2020; Meza-Figueroa et al., 2020). Mean levels of Zr, Pb, As, Zn, Cu, and Ti in studied settled dust in roofs were higher than the geochemical background concentrations reported by Taylor (1964), denoting its anthropogenic origin (Rahman et al., 2021).

Agricultural soils are generally enriched with metals due to excessive use of fertilizers and pesticides, wastewater irrigation, and atmospheric deposition (Alengebawy et al., 2021; Avendaño et al., 2021; Baltas et al., 2020). The variation coefficients (CV) expressed as percentage for Pb, As, and Zn were 84.2%, 48.2, and 42.8, respectively (Table 2). After comparing the mean concentration of metals between active and abandoned agricultural fields by the Kruskal-Wallis test (Table 3), no significant differences were found for the study metals (except Zr and Ti, $p < 0.05$). Differences between Zr and Ti can be attributed to variation in the parental source of the soils. In some of the abandoned fields, the concentration ranges of Pb, As, and Cu were higher than those found in active agricultural fields (Table 2) and mainly concentrated in sites S4 (43.5 mg kg^{-1}, 32.1 mg kg^{-1}, 76.8 mg kg^{-1}, respectively) and S9 (48.8 mg kg^{-1}, 31.5 mg kg^{-1}, 76.3 mg kg^{-1}, respectively) (Table S2). Table 2 shows metal concentrations reported for agricultural soils in various parts of the world. Most of the data from our study are similar for most of the elements reported. Iron and Mn present high values, Mn only comparable to those reported in Greece.

Pesticide concentrations in agricultural soils and dust settled on roofs

In the study sites, at least two pesticides were detected simultaneously in soils and dust settled on the roofs. In soils (Table 4), the identified pesticides were DDE (90%), aldrin (60%), endosulfan (60%), DDT (60%), and mirex (60%). The highest mean levels corresponded to DDE (12.1 μg kg^{-1}), endosulfan 4.6 μg kg^{-1}), and mirex (3.5 μg kg^{-1}), while endrin showed the lower mean levels (2 μg kg^{-1}). DDT is a highly persistent compound in the environment, so it can remain in the soil for 20 to 30 years, during which time it slowly degrades to DDE and DDD under anaerobic and aerobic conditions, respectively (Chen et al., 2021; Tzanetou & Karasali, 2022). The relationship between DDT, DDE, and DDD is a useful tool for distinguishing from the historical and recent use of this pesticide. DDT/(DDE+DDD) values >1 indicate recent use, while values less than 1 suggest historical use (Miglioranza et al., 2021). In this study, the mean DDT ratio (0.13) found in the abandoned files suggests that the accumulation of DDT in soils may result of its application in past decades. The mean DDT ratio for active fields was 2.8-fold higher than in abandoned sites; this behavior may relate to the intensive past use of DDT for wheat and cotton crops and by the health sector in campaigns against malaria.

In settled dust roof samples (Table 4), the most frequent pesticides were aldrin (84.6%), DDE (69.2%), and γ-chlordane (61.5%). The higher mean levels of pesticides in dust settled on the roof corresponded to methoxychlor (141.6 μg kg^{-1}), endrin (97.2 μg kg^{-1}), and DDT (44.5 μg kg^{-1}), meanwhile, lindane showed the lowest mean levels (0.89 μg kg^{-1}). The mean DDT ratio was 1.05, indicating its past use.

DDT was massively applied between 1945 and 1955; however, later evaluations demonstrated the negative characteristics of DDT, mainly its persistence and bioaccumulation. In the 1960s, it was found that DDT and its metabolites induce environmental damage and affect the health of organisms. In 1972, the use of DDT was banned in several countries because of the damage it causes to life. In Mexico, DDT production was stopped in 1997, and its use was discontinued in 2000. Therefore, the presence of DDT and DDE in settled dust samples collected in roofs in Hermosillo city is most likely related to the emission and dust transport by wind from the nearby agricultural areas, but particularly, from abandoned fields where pesticides were intensively applied.

Source identification metals-pesticides in agriculture soils and dust roofs

In this study, PCA was applied to aid in the identification of pollution sources in settled dust in roofs. Table 5 shows the Spearman correlation matrix for metals, metalloids, and pesticides in agricultural soils and dust deposited on roofs. In agricultural soils, Pb and As are correlated with most of the metals studied. In roof dust samples, metals and metalloids are correlated with Fe, Mn, and Ti. To better understand these correlations, we used PCA to reduce database dimensions. Table S3 shows that 87% of the cumulative variance for agricultural soils is represented in four components—F1 (39.5%), F2 (21.9%), F3 (14.5%), and F4 (11.1%). The geochemical signatures for each component are shown in Table S4 as follows: F1 is characterized by the association of endosulfan, DDD,

Table 4 Pesticide content in agricultural soils and settled dust in roofs. Concentrations in μg kg^{-1}

Sample	LIN	HEPT	ALD	HEP-EP	γ-CHLOR	ENDO	DDE	ENDR	DDD	DDT	MET	MRX
Agricultural soils												
S1	<LOD	<LOD	1.59	1.96	<LOD	2.95	4.07	3.93	<LOD	<LOD	<LOD	4.9
S2	2.57	3.96	3.96	<LOD	0.52	1.95	2.39	<LOD	<LOD	2.21	<LOD	3.82
S3	<LOD	<LOD	<LOD	<LOD	<LOD	<LOD	7.49	<LOD	<LOD	1.04	<LOD	<LOD
S4	<LOD	<LOD	1.42	<LOD	2.67	7.13	35.34	<LOD	2.35	4.94	8.26	3.68
S5	<LOD	1.22	1.06	3.34	2.31	3.26	25.92	<LOD	<LOD	<LOD	1.5	1.58
S6	<LOD	<LOD	<LOD	<LOD	<LOD	<LOD	1.79	<LOD	<LOD	<LOD	<LOD	2.34
S7	<LOD	<LOD	<LOD	<LOD	<LOD	<LOD	8.33	<LOD	<LOD	1.13	<LOD	<LOD
S8	<LOD	<LOD	<LOD	<LOD	<LOD	<LOD	4.57	0.05	<LOD	<LOD	<LOD	<LOD
S9	<LOD	<LOD	2.67	0.96	<LOD	8.51	18.53	<LOD	<LOD	1.47	<LOD	4.54
S10	<LOD	<LOD	1.7	2.56	2.56	3.61	<LOD	<LOD	<LOD	0.72	<LOD	<LOD
Settled dust in roofs												
R1	<LOD	<LOD	15.13	<LOD	2.09	<LOD	<LOD	<LOD	<LOD	<LOD	<LOD	<LOD
R2	<LOD	25.96	134.37	<LOD	<LOD	55.55	365.43	770.46	141.15	365.43	478.49	136.27
R3	<LOD	<LOD	2.67	<LOD	<LOD	<LOD	7.35	<LOD	<LOD	<LOD	<LOD	<LOD
R4	1.01	0.77	4.63	<LOD	<LOD	<LOD	3.26	<LOD	<LOD	<LOD	<LOD	<LOD
R5	<LOD	<LOD	<LOD	<LOD	<LOD	<LOD	<LOD	<LOD	<LOD	<LOD	<LOD	<LOD
R6	<LOD	<LOD	6.83	<LOD	1.44	<LOD	2.65	<LOD	<LOD	6.73	6.41	<LOD
R7	<LOD	<LOD	2.63	<LOD	0.90	<LOD	6.76	14.52	0.94	<LOD	<LOD	<LOD
R8	<LOD	<LOD	2.67	<LOD	3.41	0.88	7.35	32.91	2.75	4.13	24.59	10.21
R9	<LOD	<LOD	<LOD	<LOD	<LOD	<LOD	<LOD	<LOD	<LOD	<LOD	<LOD	<LOD
R10	<LOD	<LOD	<LOD	<LOD	<LOD	<LOD	<LOD	<LOD	<LOD	<LOD	<LOD	<LOD
R11	0.78	<LOD	4.71	<LOD	2.07	0.61	6.22	<LOD	<LOD	<LOD	<LOD	<LOD
R12	<LOD	<LOD	0.91	<LOD	<LOD	<LOD	7.35	<LOD	<LOD	<LOD	<LOD	10.21
R13	<LOD	<LOD	4.43	<LOD	1.92	0.55	3.76	35.66	3.05	<LOD	<LOD	5.30
R14	<LOD	<LOD	<LOD	<LOD	<LOD	<LOD	<LOD	<LOD	<LOD	<LOD	541.30	56.08
R15	<LOD	<LOD	8.04	<LOD	2.63	1.31	5.76	99.61	4.25	7.81	10.49	<LOD
R16	<LOD	<LOD	3.20	<LOD	2.66	<LOD	3.73	12.57	<LOD	3.88	30.59	4.55
R17	<LOD	<LOD	0.90	<LOD	<LOD	0.45	<LOD	<LOD	1.39	1.50	38.43	<LOD
R18	<LOD	0.92	2.2	<LOD	1.57	<LOD	<LOD	1.72	<LOD	<LOD	2.27	<LOD
R19	<LOD	<LOD	0.74	<LOD	1.04	<LOD	3.90	13.98	0.88	<LOD	<LOD	4.15
R20	<LOD	<LOD	0.48	<LOD	0.52	<LOD	1.99	<LOD	<LOD	<LOD	<LOD	<LOD
R21	<LOD	<LOD	4.75	<LOD	<LOD	0.85	13.53	15.65	1.31	<LOD	<LOD	<LOD
R22	<LOD	<LOD	1.03	<LOD	1.12	0.48	<LOD	10.85	<LOD	<LOD	<LOD	<LOD
R23	<LOD	<LOD	1.73	<LOD	1.67	<LOD	1.88	<LOD	<LOD	<LOD	<LOD	<LOD
R24	<LOD	<LOD	0.81	<LOD	1.05	<LOD	1.95	<LOD	<LOD	4.20	<LOD	<LOD
R25	<LOD	<LOD	6.67	<LOD	3.52	0.82	4.46	16.78	<LOD	2.21	<LOD	<LOD
R26	<LOD	<LOD	5.30	1.82	2.09	0.91	3.81	80.37	0.62	4.68	<LOD	<LOD

LIN lindane, *HEPT* heptachlor, *ALD* aldrin, *HEP-EP* heptachlor epoxide, *γ-CHLOR* γ-chlordane, *ENDO* endosulfan, *DDE* p,p′-dichlorodiphenyl-dichloroethylene, *ENDR* endrin, *DDD* p,p′-dichlorodiphenyl-dichloroethane, *DDT* p,p′-dichlorodiphenyl-trichloroethane, *MET* methoxychlor, *MRX* mirex, *LOD* limit of detection

mirex, Zr, Pb, As, Zn, Cu, Fe, and Mn. F2 shows the following related variables—DDT, endrin, V, and Ti. F3 shows an association of γ-chlordane and methoxychlor. Finally, F4 shows aldrin-DDE linked.

Table S3 also shows that 75% of the cumulative variance for dust settled in roofs was explained by four components—F1 (37.2%), F2 (20.6%), F3 (9.9%), and F4 (7.2%). Table S4 explains the

following associations per component—F1 (DDE-DDD-mirex-Zr-Pb-Zn-Cu-Fe- Mn-V-Ti) most likely related to dust impacted by vehicular traffic and pesticides.

F2 (aldrin-endosulfan-endrin-DDT-As) is related to agricultural sources, potentially abandoned fields. F3 (γ-chlordane) is possibly related to more recent agricultural activities and F4 (methoxychlor). We also conducted a PCA for all studied samples (soils and dust), and the results are shown in Fig. 2. Three groups are defined as follows: (i) association of metals possibly related to a mixture of traffic and agricultural sources (DDE, mirex, Cu, V, Ti, Mn, Fe, Zr, As) and linked cases (samples, Table S5) are shown in color red in Fig. 3. These findings are consistent with those reported the literature, which mentions that metals such As, Cr, Pb, Cu, Ni, Zn, and Mn appear in many pesticide formulations produced/applied around the world (Avendaño et al., 2021; Defarge et al., 2018). DDT and mirex agrochemicals were intensively used for to control insects in agriculture (Chen et al., 2021). Therefore, is possible that these groups of compounds may have two sources: vehicular traffic and agricultural activities. A second group (ii) aldrin-endrin, γ-chlordane, DDT, and DDD is related to agricultural activities and related samples shown in color blue in Fig. 3. A third group (iii) endosulfan-Zn-Pb is shown in yellow color in the same figure.

Assuming that the dust is transported by the wind without further chemical reactions, the signature determined by the PCA for agricultural soils should be preserved. The group of aldrin-endrin, γ-chlordane, and DDT was widely used in HCA. There are other agriculture areas close to Hermosillo, with less surface of production which may also contribute to the transport and settlement of metals and pesticides in the urban area of the city, most of the pesticides reported in the soils by Leal et al. (2014) in HCA were also detected in the dust deposited on the roofs of Hermosillo, which strengthens these results; however, more research is needed.

HYSPLIT forward trajectory model

The HYSPLIT forward trajectory was applied to study the dust transport trend of HCA fields. Sites S1, S3, S4, S5, and S8 were used as the starting point for the trajectory model since these sites had the highest percentages of silt and clay. Through these trajectories (Fig. 3), it is clearly observed that dust crosses the city of Hermosillo from west to east: S1 from SW to WE, S3 from NW to WE, S4 from SW to WE, and S8 from SW to E, demonstrating the influence of the agricultural activity of the HCA in the nearby rural communities and in the urban area of Hermosillo.

According to the results of metals in soils, the distribution of these contaminants is not uniform throughout the area due to the great variability of factors involved in their dispersion, such as the urban topography of the city (Del Río-Salas et al., 2012), the size of the dust particles (Péterfalvi et al., 2018; Singh et al., 2021), and wind direction and speed (Wang et al.,

Table 5 Spearman correlation matrix of studied samples. The gray shaded area corresponds to agricultural soils; the white area are samples of dust deposited on school roofs. Values different from zero at alpha = 0.05 significance level are in bold

	ALD	γ-CHLOR	ENDO	DDE	ENDR	DDD	DDT	MET	MRX	Zr	Pb	As	Zn	Cu	Fe	Mn	V	Ti
ALD	**1**	**0.503**	**0.576**	**0.529**	**0.523**	0355	**0.499**	0.155	-0.016	-0.123	0.208	-0.136	0.254	-0.076	-0.183	0.160	-0.152	-0.028
γ-CHLOR	0.430	**1**	0.343	0.113	**0.444**	0.087	**0.391**	0.071	-0.022	-0.098	0.050	0.148	0.201	-0.040	-0.165	0.090	-0.094	-0.039
ENDO	**0.742**	0.585	**1**	**0.496**	**0.747**	**0.688**	**0.523**	0.234	0.147	-0.040	0.323	-0.285	0.270	0.252	0.173	0.180	0.269	0.101
DDE	-0.119	0.157	0.344	**1**	**0.542**	**0.504**	0.287	0.002	0.338	0.191	**0.410**	-0.067	0.212	0.322	0.298	**0.536**	0.370	0.342
ENDR	-0.094	-0.390	-0.192	-0.182	**1**	**0.752**	**0.471**	0.223	0.325	0.118	0.334	-0.059	**0.413**	0.321	0.214	0.217	0.195	0.142
DDD	0.060	0.588	0.419	0.522	-0.166	**1**	**0.407**	0.338	0.342	0.056	**0.490**	-0.197	**0.491**	0.337	0.300	0.160	**0.437**	0.098
DDT	0.445	0.356	0.387	0.356	-0.535	0.539	**1**	**0.557**	0.150	-0.044	**0.467**	-0.017	0.310	0.224	0.126	0.168	0.285	0.122
MET	0.009	**0.702**	0.464	**0.701**	-0.247	**0.745**	0.201	**1**	**0.480**	0.083	0.003	0.329	0.333	0.340	0.212	0.314	0.314	0.166
MRX	**0.635**	-0.004	0.506	0.100	0.201	0.180	0.197	0.107	**1**	0.121	0.365	-0.135	**0.421**	0.380	**0.421**	**0.405**	**0.493**	0.318
Zr	0.000	0.123	-0.150	**-0.697**	0.216	-0.029	-0.575	-0.199	-0.088	**1**	**0.428**	**0.650**	0.265	**0.813**	**0.815**	**0.737**	0.142	**0.892**
Pb	0.209	-0.194	0.323	0.252	0.026	0.411	0.367	0.061	**0.677**	-0.485	**1**	0.099	**0.692**	**0.621**	**0.656**	**0.565**	**0.459**	**0.571**
As	0.331	0.055	0.381	0.430	-0.069	0.522	0.619	0.234	0.588	**-0.697**	**0.865**	**1**	-0.012	**0.541**	**0.399**	**0.454**	0.095	**0.461**
Zn	0.056	-0.116	0.156	0.079	-0.069	0.406	0.269	0.061	0.500	-0.358	**0.926**	**0.794**	**1**	0.380	**0.417**	0.360	**0.400**	0.338
Cu	0.144	-0.041	0.319	0.345	-0.069	0.522	0.400	0.234	0.582	-0.552	**0.963**	**0.915**	**0.952**	**1**	**0.885**	**0.750**	**0.509**	**0.819**
Fe	0.050	-0.130	0.138	0.091	0.121	0.406	0.113	0.138	**0.638**	-0.224	**0.902**	**0.745**	**0.952**	**0.915**	**1**	**0.811**	**0.505**	**0.881**
Mn	0.075	-0.130	0.188	0.139	0.026	0.406	0.181	0.138	0.625	-0.321	**0.939**	**0.782**	**0.976**	**0.952**	**0.988**	**1**	**0.441**	**0.864**
V	-0.244	-0.061	-0.169	-0.067	0.545	0.058	-0.619	0.242	0.294	0.273	0.190	0.091	0.321	0.261	0.539	0.442	**1**	0.267
Ti	-0.188	0.089	-0.125	-0.248	0.545	0.058	**-0.707**	0.242	0.213	0.600	-0.055	-0.236	0.067	-0.030	0.309	0.200	**0.891**	**1**

ALD aldrin, *γ-CHLOR* γ-chlordane, *ENDO* endosulfan, *DDE* p,p′-dichlorodiphenyl-dichloroethylene, *ENDR* endrin, *DDD* p,p′-dichlorodiphenyl-dichloroethane, *DDT* p,p′-dichlorodiphenyl-trichloroethane, *MET* methoxychlor, *MRX* mirex, *LOD* limit of detection

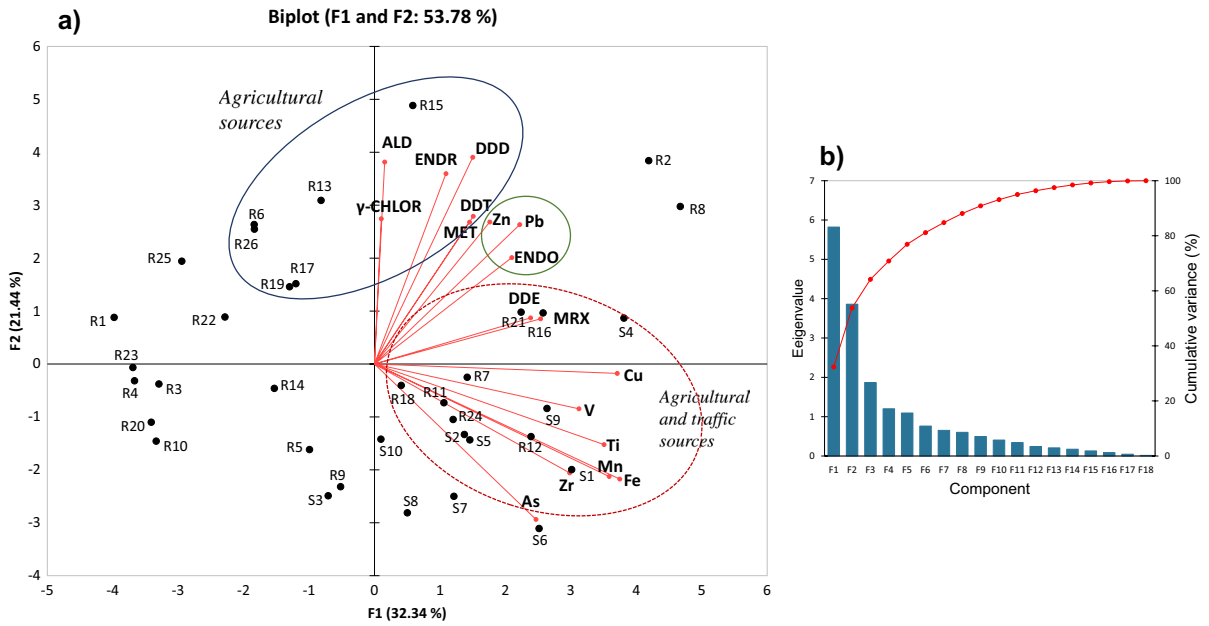

Fig. 2 Principal component analysis of pollutants and samples. **a** Agricultural soils and settled dust in roofs and **b** scree plot of PCA

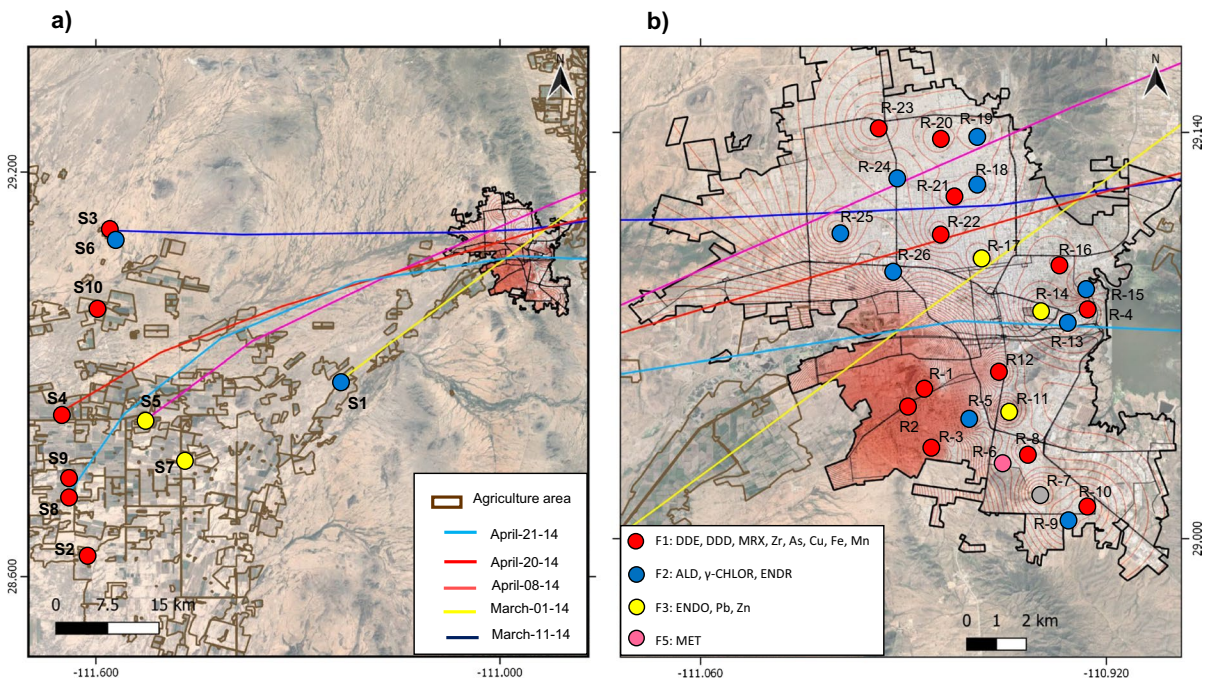

Fig. 3 HYSPLIT particle forward trajectories from **a** agricultural fields and **b** PCA mapping

2019; Zhang et al., 2018). In this sense, it is important to point out the importance of ≤ 20 μm particles in soils. The transport and deposition of these particle size take place at a higher altitude than larger particles. Therefore, according to the presence of metals in soils/dust and the determined trajectories, it is likely that

significant levels of transported metals by dust may settled on roofs buildings of Hermosillo city, especially in the zones where the HYSPLIT trajectories converge.

To identify the source of metals settled on the roof, the presence of pesticides was also employed as tracers. For example, Fig. 3 shows the spatial distribution of DDD (shaded red). The highest concentrations of DDD corresponded to the area where the HYSPLIT trajectories converge (especially sites S1, S3, and S5). Most of the city's surface area is impervious, so local soil resuspension processes are very limited; additionally, the city has no cultivated areas; therefore, considering the results of the air mass forward trajectories (Fig. 3), the accumulation of pesticides in the dust deposited on the roofs could be related to the atmospheric transport from HCA. Similar results were found using backward trajectory analysis at rooftop sampling points, showing trajectories related to agricultural fields (Fig. S1).

The occurrence of pesticides in the dust deposited on the roofs of the city of Hermosillo clearly indicates the relevance of agriculture impacts in the area. In Northwestern Mexico occurs other important agricultural

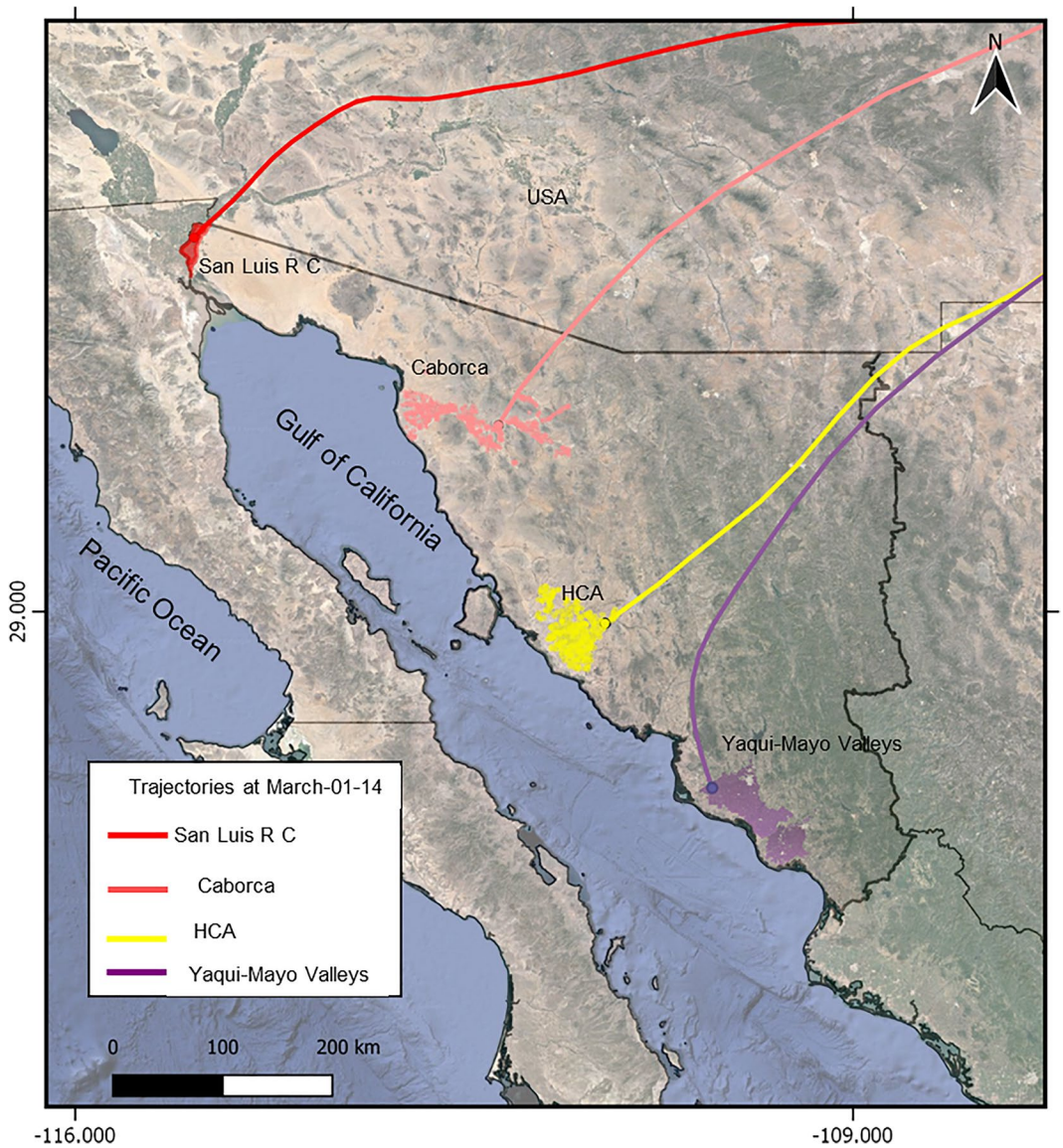

Fig. 4 Forward trajectories originated from the most important agriculture areas in Sonora, Mexico

areas such Yaqui and Mayo Valleys with a legacy of pesticide and metals. Nevertheless, the results of the air mass forward trajectories (Fig. 4) indicated that the metals and pesticides detected in Hermosillo are a direct consequence of the agriculture carried out in HCA.

It is important to note that there are other agricultural areas near Hermosillo that could also be contributing to the metal content in the dust. Figure 4 shows the HYSPLIT advance trajectories on March 1–14 for agricultural areas of San Luis Rio Colorado, Caborca, and the Yaqui and Mayo valleys. The results indicate that during pre-monsoon season, these agricultural areas have an influence on the neighboring state of Chihuahua, and even it is clearly observed its influence over the USA (Arizona), but not in the city of Hermosillo. Although these agricultural areas are the most important in terms of production, there are other areas on smaller scale for which their emission range and trajectories remain unknown. Despite the main objective of this research is the identification of possible sources of metals in HCA, the use of pesticides proved to be a useful tool for this purpose. Although several authors have used metals as pollution tracers, the results of this research suggest that pesticides may be better tracers than metals; however, metals and pesticides in conjunction with air mass forward trajectories provide better results.

Conclusion

This study is the first performed in Mexico that assesses the transport of multiple metals in dust from an agricultural area with several abandoned agricultural fields.

According to PCA analysis, three groups are defined as follows: (i) a mixture of traffic and agricultural sources (DDE, mirex, Cu, V, Ti, Mn, Fe, Zr, As), (ii) a group related to agricultural activities (aldrin-endrin, γ-chlordane, DDT, DDD), and (iii) and association of endosulfan-Zn-Pb related to mix sources including tire wear.

The results of the air mass forward trajectories clearly indicate the long-range transport of metals in dust and reveal the influence of agriculture in the neighboring states of Chihuahua and Arizona (USA). Based on the results of this research, HCA agricultural fields are a major route of exposure to metals related to the historical and intensive agricultural activity, and dust from abandoned agricultural fields is deposited in nearby settlements. Therefore, it is recommended to improve agricultural practices to reduce the emission of particulate matter, and more detailed studies determining emission rates are needed to assess the impact that these emissions may have on human health.

Acknowledgements We thank S. Leal for field support and B. Gonzalez-Grijalva for the technical assistance. We appreciated the support of doctoral scholarship to J. Bracamonte-Terán by CONAHCYT.

Author contribution Bracamonte-Terán J: Formal analysis, methodology, validation, writing the first draft. Meza-Figueroa D: Conceptualization, visualization, funding acquisition, resources, writing original draft, writing- review & editing. García-Rico L: Supervision, visualization, investigation, writing original draft, writing - review & editing. Schiavo B: Methodology, formal analysis, review & editing. Meza-Montenegro M: Methodology, resources, review & editing. Valenzuela-Quintanar A: Methodology, validation, resources, review & editing. All authors reviewed the manuscript.

Funding This work was supported by the National Council of Humanities, Science and Technology, Mexico (Consejo Nacional de Humanidades, Ciencia y Tecnologia, CONAHCYT), through the grants PRONACES 317557 and 10261.

Data availability Data will be made available on request.

Declarations

Ethics approval and consent to participate Not applicable.

Competing interest The authors declare that they have no known competing financial interests or personal relationships that could have appeared to influence the work reported in this paper.

References

Alengebawy, A., Abdelkhalek, S. T., Qureshi, S. R., & Wang, M. Q. (2021). Heavy metals and pesticides toxicity in agricultural soil and plants: Ecological risks and human health implications. *Toxics, 9*(3), 1–34. https://doi.org/10.3390/toxics9030042

Attiya, A. A., & Jones, B. G. (2020). Assessment of mineralogical and chemical properties of airborne dust in Iraq. *SN Applied Sciences, 2*(9), 1–21. https://doi.org/10.1007/s42452-020-03326-5

Avendaño, M. C., Palomeque, M. E., Roqué, P., Lojo, A., & Garrido, M. (2021). Spatiotemporal distribution and human health risk assessment of potential toxic species in soils of urban and surrounding crop fields from an agricultural area, Córdoba, Argentina. *Environmental Monitoring and Assessment, 193*(10), 1-19. https://doi.org/10.1007/s10661-021-09358-7

Baltas, H., Sirin, M., Gökbayrak, E., & Ozcelik, A. E. (2020). A case study on pollution and a human health risk assessment of heavy metals in agricultural soils around Sinop province, Turkey. *Chemosphere, 241*, 125015. https://doi.org/10.1016/j.chemosphere.2019.125015

Bhuiyan, M. A., Karmaker, S. C., Bodrud-Doza, M., Rakib, M. A., & Saha, B. B. (2021). Enrichment, sources and ecological risk mapping of heavy metals in agricultural soils of Dhaka District employing SOM, PMF and GIS. *Chemosphere, 263*, 128339. https://doi.org/10.1016/j.chemosphere.2020.128339

Candeias, C., Freire-Ávila, P., Alves, C., Gama, C., Sequeira, C., Ferreira da Silva, E., & Rocha, F. (2021). Dust characterization and its potential impact during the 2014–2015 Fogo Volcano Eruption (Cape Verde). *Minerals, 11*, 1275. https://doi.org/10.3390/min11111275

Chalise, D., Kumar, L., & Kristiansen, P. (2019). Land degradation by soil erosion in Nepal: A review. *Soil Systems, 3*(1), 1–18. https://doi.org/10.3390/soilsystems3010012

Chen, W., Zeng, F., Liu, W., Bu, J., Hu, G., Xie, S., & Huang, H. (2021). Organochlorine pesticides in karst soil: Levels, distribution, and source diagnosis. *International Journal of Environmental Research and Public Health, 18*(21), 11589. https://doi.org/10.3390/ijerph182111589

Defarge, N., Spiroux de Vendômois, J., & Séralini, G. E. (2018). Toxicity of formulants and heavy metals in glyphosate-based herbicides and other pesticides. *Toxicology Reports, 5*, 156–163. https://doi.org/10.1016/j.toxrep.2017.12.025

Del Río-Salas, R., Ruiz, J., De la O-Villanueva, M., Valencia-Moreno, M., Moreno-Rodríguez, V., Gómez-Alvarez, A., Grijalva, T., Mendivil, H., Paz-Moreno, F., & Meza-Figueroa, D. (2012). Tracing geogenic and anthropogenic sources in urban dusts: Insights from lead isotopes. *Atmospheric Environment, 60*, 202–210. https://doi.org/10.1016/j.atmosenv.2012.06.061

Fei, X., Lou, Z. L., Xiao, R., Ren, Z., & Lv, X. (2022). Source analysis and source-oriented risk assessment of heavy metal pollution in agricultural soils in different cultivated land qualities. *Journal of Cleaner Production, 341*, 130942. https://doi.org/10.1016/j.jclepro.2022.130942

Fry, K. L., Gillings, M. M., Isley, C. F., Gunkel-Grillon, P., & Taylor, M. P. (2021). Trace element contamination of soil and dust by a New Caledonian ferronickel smelter: Dispersal, enrichment, and human health risk. *Environmental Pollution, 288*, 117593. https://doi.org/10.1016/j.envpol.2021.117593

Gallego-Hernández, A. L., Meza-Figueroa, D., Tanori, J., Acosta-Elias, M., Gonzalez-Grijalva, B., Maldonado-Escalante, F., Rochin-Wong, S., Soto-Puebla, D., Navarro-Espinoza, S., Ochoa-Contreras, R., & Pedroza-Montero, M. (2020). Identification of inhalable rutile and polycyclic aromatic hydrocarbons (PAHs) nanoparticles in the atmospheric dust. *Environmental Pollution, 260*, 114006. https://doi.org/10.1016/j.envpol.2020.1144006

González-Guzmán, R., Inguaggiato, C., Brusca, L., González-Acevedo, Z. I., & Bernard-Romero, R. (2022). Assessment of potentially toxic elements (PTEs) sources on soils surrounding a fossil fuel power plant in a semi-arid/arid environment: A case study from the Sonoran Desert. *Applied Geochemistry, 136*, 105158. https://doi.org/10.1016/j.apgeochem.2021.105158

Huang, S. W., & Jin, J. Y. (2008). Status of heavy metals in agricultural soils as affected by different patterns of land use. *Environmental Monitoring and Assessment, 139*, 317–327. https://doi.org/10.1007/s10661-007-9838-4

IPCC. (2019). Intergovernmental Panel on Climate Change. Summary for policymakers. In P. R. Shukla, J. Skea, E. Calvo Buendía, V. Masson-Delmotte, H. O. Pörtner, D. C. Roberts, P. Zhai, R. Slade, S. Connors, & R. van Diemen (Eds.), *Climate change and land: An IPCC Special Report on climate change, desertification, land degradation, sustainable land management, food security, and greenhouse gas fluxes in terrestrial ecosystems*. United Nations, IPCC ISBN 978-92-9169-154-8. https://www.ipcc.ch/srccl/

Jooybari, S. A., Peyrowan, H., Rezaee, P., & Gholami, H. (2022). Evaluation of pollution indices, health hazards and source identification of heavy metal in dust particles and storm trajectory simulation using HYSPLIT model (case study: Hendijan center dust, southwest of Iran). *Environmental Monitoring and Assessment, 194*, 107. https://doi.org/10.1007/s10661-022-09760-9

Joshi, J. R. (2021). Quantifying the impact of cropland wind erosion on air quality: A high-resolution modeling case study of an Arizona dust storm. *Atmospheric Environment, 263*, 118658. https://doi.org/10.1016/j.atmosenv.2021.118658

Katra, I. (2020). Soil erosion by wind and dust emission in semi-arid soils due to agricultural activities. *Agronomy, 10*(1), 89. https://doi.org/10.3390/agronomy10010089

Kelepertzis, E. (2014). Accumulation of heavy metals in agricultural soils of Mediterranean: Insights from Argolida basin, Peloponnese, Greece. *Geoderma, 221*, 82–90. https://doi.org/10.1016/j.geoderma.2014.01.007

Leal, S. D., Valenzuela, A. I., Gutiérrez, M. L., Bermúdez, M. C., García, J., Aldana, M. L., & Palma, S. A. (2014). Residuos de plaguicidas organoclorados en suelos agrícolas. *Terra Latinoamericana, 32*(1), 111 https://www.terralatinoamericana.org.mx/index.php/terra/article/view/14/12

Lee, P. K., Kang, M. J., Yu, S., & Kwon, Y. K. (2020). Assessment of trace metal pollution in roof dusts and soils near a large Zn smelter. *Science of the Total Environment, 713*, 136536. https://doi.org/10.1016/j.scitotenv.2020.136536

Luo, H., Guan, Q., Pan, N., Wang, Q., Li, H., Lin, J., Tan, Z., & Shao, W. (2020). Using composite fingerprints to quantify the potential dust source contributions in northwest China. *Science of the Total Environment, 742*, 140560. https://doi.org/10.1016/j.scitotenv.2020.140560

Meza-Figueroa, D., Barboza-Flores, M., Romero, F. M., Acosta-Elias, M., Hernandez-Mendiola, E., Maldonado-Escalante, F., Perez-Segura, E., Gonzalez-Grijalva, B., Meza-Montenegro, M. M., Garcia-Rico, L., Navarro-Espinoza, S., Santacruz-Gómez, K., Gallego-Hernández, A., & Pedroza-Montero, M. (2020). Metal bioaccessibility, particle size distribution and polydispersity of playground dust in synthetic lysosomal fluids. *Science of the Total Environment, 713*, 136481. https://doi.org/10.1016/j.scitotenv.2019.136481

Meza-Figueroa, D., González-Grijalva, B., Del Río-Salas, R., Coimbra, R., Ochoa-Landin, L., & Moreno-Rodríguez, V.

(2016). Traffic signatures in suspended dust at pedestrian levels in semiarid zones: Implications for human exposure. *Atmospheric Environment, 138*, 4–14. https://doi.org/10.1016/j.atmosenv.2016.05.005

Meza-Montenegro, M. M., Gandolfi, A. J., Santana-Alcántar, M. E., Klimecki, T. W., Aguilar-Apodaca, M. G., Del Río-Salas, R., & De la O-Villanueva, M., Gómez-Alvarez, A., Mendivil-Quijada, H., & Meza-Figueroa, D. (2012). Metals in residential soils and cumulative risk assessment in Yaqui and Mayo agricultural valleys, northern Mexico. *Science of the Total Environment, 433*, 472–481. https://doi.org/10.1016/j.scitotenv.2012.06.083

Meza-Montenegro, M. M., Valenzuela-Quintanar, A. I., Balderas-Cortés, J. J., Yañez-Estrada, L., Gutiérrez-Coronado, M. L., Cuevas-Robles, A., & Gandolfi, A. J. (2013). Exposure assessment of organochlorine pesticides, arsenic, and lead in children from the major agricultural areas in Sonora, Mexico. *Archives of Environmental Contamination and Toxicology, 64*(3), 519–527. https://doi.org/10.1007/s00244-012-9846-4

Miglioranza, K. S. B., Ondarza, P. M., Costa, P. G., de Azevedo, A., Gonzalez, M., Shimabukuro, V. M., Grondona, S. I., Mitton, F. M., Barra, R. O., Wania, F., & Fillmann, G. (2021). Spatial and temporal distribution of persistent organic pollutants and current use pesticides in the atmosphere of Argentinean Patagonia. *Chemosphere, 266*, 129015. https://doi.org/10.1016/j.chemosphere.2020.129015

Moreno-Rodríguez, V., Del Rio-Salas, R., Loredo-Portales, R., Briseño-Beltrán, A., Romo-Morales, D., Zepeda, J., Peña-Ortega, M., Espinoza-Maldonado, I. G., & De la O-Villanueva, M. (2020). Abandoned agricultural lands as a source of arsenic in semi-arid regions: Influence on human exposure and health risk assessment in vulnerable rural areas. *Journal of South American Earth Sciences, 104*, 102829. https://doi.org/10.1016/j.jsames.2020.102829

Moreno-Rodríguez, V., Del Río-Salas, V., Adams, D. K., Ochoa-Landin, L., Zepeda, J., Gómez-Alvarez, A., Palafox-Reyes, J., & Meza-Figueroa, D. (2015). Historical trends and sources of TSP in a Sonoran desert city: Can the North America Monsoon enhance dust emissions? *Atmospheric Environment, 110*, 111–121. https://doi.org/10.1016/j.atmosenv.2015.03.049

NMX-AA-132-SCFI-2016. (2016). Norma Mexicana. Soil sampling for metals and metalloids identification and quantification, and sample handling. Secretaría de Economía-Diario Oficial de la Federación, México city. http://www.economia-nmx.gob.mx/normas/nmx/2010/nmx-aa-132-scfi-2016.pdf

Ochoa-Noriega, C., Velasco-Muñoz, J. F., Aznar-Sánchez, J. A., & López-Felices, B. (2022). Analysis of the acceptance of sustainable practice in water management for the intensive agriculture of the Costa de Hermosillo (Mexico). *Agronomy, 12*, 154. https://doi.org/10.3390/agronomy12010154

Péterfalvi, N., Keller, B., & Magyar, M. (2018). PM10 emission from crop production and agricultural soils. *Agrokémia és Talajtan, 67*(1), 143–159. https://doi.org/10.1556/0088.2018.67.1.10

Pi, H., Webb, N. P., Lei, J., & Li, S. (2022). Soil loss and PM10 emissions from agricultural fields in the Junggar basin over the past six decades. *Journal of Soil and Water Conservation, 77*(2), 113–125. https://doi.org/10.2489/jswc.2022.00018

Pozzer, A., Tsimpidi, A. P., Karydis, V. A., de Meij, A., & Lelieveld, J. (2017). Impact of agricultural emission reductions on fine particulate matter and public health. *Atmospheric Chemistry and Physics, 17*(20), 12813–12826. https://doi.org/10.5194/acp-17-12813-2017

Qishlaqui, A., & Moore, F. (2007). Statistical analysis of accumulation and sources of heavy metals occurrence in agricultural soils of Khoshk River banks, Shiraz, Iran. American-Eurasian. *Journal of Agriculture and Environmental Sciences, 2*(5), 565–573 http://www.idosi.org/aejaes/jaes2(5)/17.pdf

Rahman, M. S., Kumar, P., Ullah, M., Jolly, Y. N., Akhter, S., Kabir, J., Begum, B. A., & Salam, A. (2021). Elemental analysis in surface soil and dust of roadside academic institutions in Dhaka City, Bangladesh and their impact on human health. *Environmental Chemistry and Ecotoxicology, 3*, 197–208. https://doi.org/10.1016/j.enceco.2021.06.001

Ramirez, H. N. B., Aparicio, V. C., & Mendez, M. J. (2021). First evidence of glyphosate and aminomethylphosphonic acid (AMPA) in the respirable dust (PM10) emitted from unpaved rural roads of Argentina. *Science of the Total Environment, 773*, 145055. https://doi.org/10.1016/j.scitotenv.2021.145055

Salazar-Adams, A., Moreno-Vázquez, J. L., & Lutz-Ley, A. N. (2012). Agricultura y manejo sustentable del acuífero de la Costa de Hermosillo. *Región y Sociedad, 3*, 155–179. https://doi.org/10.22198/rys.2012.3.a411

SIAP. (2021). Servicio de Información Agroalimentaria y Pesca. Anuario Estadístico de la Producción Agrícola: Producción Agrícola 2010-2020. Secretaría de Agricultura y Desarrollo Rural. México. https://www.google.com/url?q=https://nube.siap.gob.mx/cierreagricola/&source=gmail-imap&ust=1664568198000000&usg=AOvVaw00TpReb1JMoLJc12YwTkdK

Singh, T., Ravindra, K., Beig, G., & Mor, S. (2021). Influence of agricultural activities on atmospheric pollution during post-monsoon harvesting seasons at a rural location of Indo-Gangetic Plain. *Science of the Total Environment, 796*, 148903. https://doi.org/10.1016/j.scitotenv.2021.148903

Spada, N. J., McNally, A. M., Gill, T. E., Best, H. Q., Wells, A. M., & Longcore, T. (2023). Fugitive gypsum dust deposition on a neighboring wildlife refuge, Antioch Dunes, California, USA. *Journal of the Air & Waste Management Association*. https://doi.org/10.1080/10962247.2023.2254267

Sprigg, W. A., Nickovic, S., Galgiani, J. V., Pejanovic, G., Petkovic, S., Vujadinovic, M., Vukovic, A., Dacic, M., Di Biase, S., Prasad, A., & El-Askary, H. (2014). Regional dust storm modeling for health services: The case of valley Fever. *Aeolian Research, 14*, 53–73. https://doi.org/10.1016/j.aeolia.2014.03.001

Taylor, S. R. (1964). Abundance of chemical elements in the continental crust: a new table. *Geochimica et Cosmochimica Acta, 28*(8), 1273. https://doi.org/10.1016/0016-7037(64)90129-2

Tóth, G., Hermann, T., Da Silva, M. R., & Montanarella, L. (2016). Heavy metals in agricultural soils of the European Union with implications for food safety. *Environment International, 88*, 299–309. https://doi.org/10.1016/j.envint.2015.12.017

Tzanetou, E. N., & Karasali, H. (2022). A comprehensive review of organochlorine pesticide monitoring in agricultural soils: The silent threat of a conventional agricultural past. *Agriculture, 12*(*5*), 728. https://doi.org/10.3390/agriculture12050728

USEPA. (2007). United States Environmental Protection Agency. Method 6200. Field portable X-ray fluorescence spectrometry for the determination of elemental concentrations in soil and sediment. Washinton, DC, USA. Environmental Protection Agency. https://www.epa.gov/sites/default/files/2015-12/documents/6200.pdf

Vimic, A. V., Cvetkovic, B., Giannaros, T. M., Shahbazi, R., Kashani, S. S., Prieto, J., Kotroni, V., Lagouvardos, K., Pejanovic, G., Petkovic, S., Nickovic, S., Mandic, M. V., Basart, S., Boloorani, A. D., & Terradellas, E. (2021). Numerical simulation of Tehran dust storm on 2 June 2014: A case study of agricultural abandoned lands as emission sources. *Atmosphere, 12*(8), 1054. https://doi.org/10.3390/atmos12081054

Wagari, M., & Tamiru, H. (2021). RUSLE model based annual soil loss quantification for soil erosion protection: A case of Fincha Catchment, Ethiopia. *Air, Soil and Water Research, 14*, 1–12. https://doi.org/10.1177/11786221211046234

Wang, J., Xie, X., & Fang, C. (2019). Temporal and spatial distribution characteristics of atmospheric particulate matter (PM10 and PM2.5) in Changchun and analysis of its influencing factors. *Atmosphere, 10*(11), 651. https://doi.org/10.3390/atmos10110651

Wang, Y., Guo, G., Zhang, D., & Lei, M. (2021). An integrated method for source apportionment of heavy metal(loid)s in agricultural soils and model uncertainty analysis. *Environmental Pollution, 276*, 116666. https://doi.org/10.1016/j.envpol.2021.116666

Zeb, B., Alam, K., Ditta, A., Ullah, S., Ali, H., Ibrahim, M., & Salem, M. Z. M. (2022). Variation in coarse particulate matter (PM10) and its characterization at multiple locations in the semiarid region. *Frontiers in Environmental Science, 10*. https://doi.org/10.3389/fenvs.2022.843582

Zepeda, Q. D. S., Loeza, R. C. M., Munguía, V. N. E., Esquer, P. J., & Velazquez, C. L. E. (2018). Sustainability strategies for coastal aquifers: A case study of the Hermosillo Coast aquifer. *Journal of Cleaner Production, 195*, 1170–1182. https://doi.org/10.1016/j.jclepro.2018.05.191

Zhang, B., Jiao, L., Xu, G., Zhao, S., Tang, X., Zhou, Y., & Gong, C. (2018). Influences of wind and precipitation on different-sized particulate matter concentrations (PM2.5, PM10, PM2.5–10). *Meteorology and Atmospheric Physics, 130*(3), 383–392. https://doi.org/10.1007/s00703-017-0526-9